

# On the Modeling and State Estimation for Dynamic Power System

A. Thabet, M. Boutayeb, M. N. Abdelkrim

**Abstract**—This paper investigates a method for the state estimation of nonlinear systems described by a class of differential-algebraic equation (DAE) models using the extended Kalman filter. The method involves the use of a transformation from a DAE to ordinary differential equation (ODE). A relevant dynamic power system model using decoupled techniques will be proposed. The estimation technique consists of a state estimator based on the EKF technique as well as the local stability analysis. High performances are illustrated through a simulation study applied on IEEE 13 buses test system.

**Keywords**—Power system, Dynamic decoupled model, Extended Kalman Filter, Convergence analysis, Time computing.

## NOMENCLATURE

$M$	Inertia constant of the generator
$D$	Damping constant of the generator
$\delta$	mechanical rotor angle of the rotating machine
$\omega$	mechanical angular velocity
$\omega_s$	electrical angular velocity
$P_M$	Mechanical power input
$P_p, Q_i$	Nodal active and reactive power
$P_{c,d}$	Transit power
$Y_{bus}$	Nodal admittance matrix
$G_{ij}, B_{ij}$	real and imaginary terms of bus admittance matrix corresponding to $i$ th row and $j$ th column
$N$	Total number of system buses
$n_g$	Number of generator buses
$n_l$	Number of load buses
$P_{Gi}$	Electrical power supplied by the generator
$\theta_i, U_i$	Phase and voltage at bus $i$
$\Delta\theta_i, \Delta U_i$	Variation of phase and voltage
$r, x$	Resistance and inductive reactance of line

## I. INTRODUCTION

**D**YNAMIC state estimation plays a basic and very important role in modern industries. Particularly in the power systems, state estimation generates critical input data for driving other operation functions including real-time security monitoring, load-forecasting, economic dispatch, load-frequency control, etc.

Hence, an efficient and accurate dynamic state estimation is

Assem Thabet and M.N. Abdelkrim are with Research Unit Modeling, Analysis and Control of Systems (MACS), University of Gabes, Tunisia (e-mail: assem.thabet@yahoo.fr, naceur.abdelkrim@enig.rmu.tn).

Boutayeb Mohamed is with Research center of automatic of Nancy (CRAN), CRAN-LONGWY- IUT Henri Poincare, France (e-mail: Mohamed.Boutayeb@iut-longwy.uhp-nancy.fr).

a prerequisite for an efficient and reliable operation of power system [1].

State estimation in power system has mainly focused on Static State Estimation (SSE) from redundant measurement [2] [3]. However, to oversee an electrical power system in efficient, economic and secure manner, it is most important to be acquainted with the different dynamics states and then it's Dynamic State Estimation (DSE) in electric power system, which appries of the aforesaid information.

In designing a DSE, it is important to consider all algebraic and dynamic variables (bus voltages/phases and generators variables). The existing models are based on reducing the size of the model (linearized DAE) [4], linearization of the model [5]. To override the limitations of the existing models, a relevant and new model has been considered in this paper to model the dynamics of the power system based on the nonlinear DAE models proposed in [6]. We show that we can always rewrite the system with a nonlinear DAE form with explicit ODE to facilitate its implementation and operation.

After validation of a robust dynamic model, it is extremely important to consider a robust estimator which reflects a reliable image in the terms of capacity as for estimation, robustness and stability. A large number of existing methods are based on:

- The power system is considered as a quasi-static variables (voltages magnitudes and angles at network buses) and then applying a tracking estimator [7].
- Definition of spaces of linear combinations and their algebraic complement for the calculation of the observer gains [8].
- The Kalman filter (by linearizing the DAE or ODE model [9]) [1], [10] with different resolution techniques (by varying the algorithm of resolution such as Square Root Filter Algorithm [11] or changing the weight vector [12]).

Most methods are based on the Kalman Filter for the reason of the complexity of the model [13] [14]. The advantages of the EKF are its simplicity, the fact that it is a recursive algorithm and so its computational load is modest [15] [16]. The EKF is suitable for real-time industrial-scale applications [17] with the development of the Digital Signal Processor devices.

The aim of this work is to show how a simple EKF algorithm can solve the dynamic state estimation problem for power systems. Indeed, the description of the network by a dynamic model leads us to have an idea about the transient behavior that plays a central role in monitoring and controlling design. To do so, through an IEEE 3-buses

example, we show that the dynamic model is always written as a nonlinear DAE. To develop useful and simple state estimator, we transform the obtained model into an augmented one written as a system of ordinary differential equations. Furthermore, to reduce the computational requirements and numerical instabilities, we show in the proposed decoupled dynamic model that the inverse of the Jacobian matrix can be approximated by the inverse of a block diagonal matrix using two sub-matrices of small dimensions. Thus, we propose a state estimator based on the EKF with a study of stability analysis. In the last section, numerical simulations applied on the IEEE 13-buses test system will show the relevance and efficiency of the proposed approaches.

## II. DYNAMIC POWER SYSTEM MODEL

The dynamics of a power system can be modeled with a combination of nonlinear differential equations and nonlinear algebraic equations. These sets of equations are often solved separately in different analysis techniques. The solution is accomplished in an iterative way, with the important feature that all the desired system characteristics are included. The general form of the DAE model is given as:

$$\begin{cases} \dot{x}_d(t) = F_d(x_d(t), x_a(t), u(t)) \\ 0 = g(x_d(t), x_a(t)) \\ y(t) = h(x_d(t), x_a(t)) \end{cases} \quad (1)$$

with:  $x_d(t) \in \mathbb{R}^{n_d}$  and  $x_a(t) \in \mathbb{R}^{n_a}$  are respectively dynamic and algebraic states,  $F_d(t) \in \mathbb{R}^{n_d}$  a function representing the nonlinear differential equations,  $g(\cdot) \in \mathbb{R}^{n_a}$  represents the nonlinear algebraic constraints (equations),  $u(t) \in \mathbb{R}^p$  the control and  $y(t) \in \mathbb{R}^m$  the output system. The problem with the system (1) is that  $\dot{x}_d(t)$  does not appear explicitly.

### A. Problem Formulation

To put out, in details, the physical dynamic power model, we will treat the case of the 3 buses test system given in Fig. 1 (with  $n_g=2$  and  $n_l=1$ ):

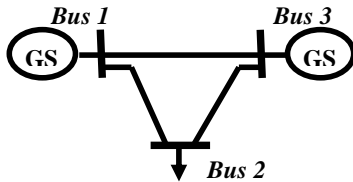


Fig. 1 3 Buses test system

We consider these assumptions [6]:

- The internal field currents are constant, providing the representation of the machine as a constant voltage behind the direct axis transient reactance.
- The mechanical power provided by the prime mover is

constant and all dynamics of the prime mover are neglected.

- All generators are rotating at synchronous speed (steady state) and are round rotors.
- All generators in the system are identical, and therefore the inertia constant ( $M_i$ ) along with the damping constant ( $D_i$ ) of each generator have the same value.
- The mechanical rotor angle is the same as the electrical phase angle of the voltage therefore  $\delta$  now refers to the electrical angle. To further simplify the notation, the transient reactance is incorporated into the system  $Y_{bus}$ , resulting in  $\theta_i$  as generator terminal voltage phase and  $V_i$  as the terminal voltage magnitude.

If we take node 1 as reference, the set of equation of this network is given by [6]:

$$\begin{cases} f_i^I : \dot{\delta} - \omega_i + \omega_s = 0 \\ f_i^{II} : \omega_i = \frac{\omega_s}{2M} (P_{M_i} - P_{G_i}(\delta, \theta, V) - D\omega_i) \\ g_i^I : P_j - P_j(\delta, \theta, V) = 0 \\ g_i^{II} : Q_j - Q_j(\delta, \theta, V) = 0 \\ y_q : P_{c,d} = P_{c,d}(\delta, \theta, V) \end{cases} \quad (2)$$

with:  $i = 1 \dots n_g - 1$ ;  $j = (n_g + 1) \dots (n_g + n_l)$ ;  $q = 1 \dots m$ ;  $c, d = 1 \dots N$ , the node 1 is taken as the reference and :

$$P_{G_i} = \sum_{j=1}^N V_i \| V_j \| [G_{ij} \cos(\delta_i - \theta_j) + B_{ij} \sin(\delta_i - \theta_j)]$$

Therefore the model (2) can be rewritten under this form:

$$\begin{aligned} F(\dot{x}, x, \beta) &= u \\ y &= h(x, \beta) \end{aligned}$$

with:  $x = [\delta_i, \omega_i, \theta_i, V_i]^T$ ,  $u = \frac{P_{M_i}}{M}$ ,  $\beta = \{Y_{bus}\}$ ,  $F(\cdot) = [f_i, g_j]^T$  and  $y = P_{c,d}$  where  $u$  and  $y$  will be respectively the control and the output of the system. The choice of transit power as output which is based on this measure is used by the Tunisian Company of Electricity and Gas. Thus for this network, the state vector and the system equations are given by (3) and (4).

$$x = [x_1 \ x_2 \ x_3 \ x_4]^T = [\delta_3 \ \omega_3 \ \theta_2 \ V_2]^T \quad (3)$$

$$\begin{cases} f^I : \dot{x}_1 = x_2 - \omega_s \\ f^{II} : \dot{x}_2 = \frac{\omega_s}{2M} (P_{M_3} - P_{G_3}(x_1, x_3, x_4) - D x_2) \\ g^I : P_2 - P_2(x_1, x_3, x_4) = 0 \\ g^{II} : Q_2 - Q_2(x_1, x_3, x_4) = 0 \\ y_1 : P_{3,2}(x_1, x_3, x_4) \end{cases} \quad (4)$$

with  $x_1$  and  $x_2$  are the dynamic variables,  $x_3$  and  $x_4$  are the algebraic variables. While using (1) the system is rewritten as:

$$\begin{cases} \dot{x}_d = \begin{pmatrix} \dot{x}_1 \\ \dot{x}_2 \end{pmatrix} = F_d(x_1, x_2, x_3, x_4, u) = [f^I, f^{II}]^T \\ g(x_1, x_2, x_3, x_4) = [g^I, g^{II}]^T = 0 \\ y(t) = P_{3,2}(x_1, x_3, x_4) \end{cases}$$

A simple diagram for the simulation of power system with model (1) is proposed, which: for the dynamic states we use a block of integration with nonlinear function ( $F_d(t)$ ) with algebraic constraints resolver under a package *SIMULINK* of *MATLAB*®. The simulation diagram is as follows (Fig. 2):

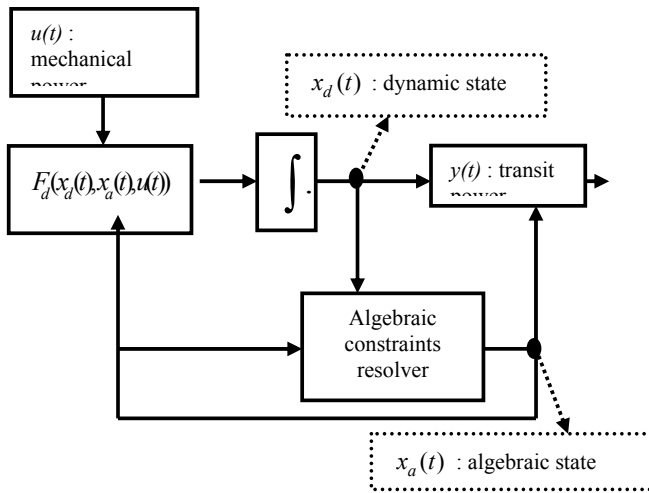


Fig. 2 Diagram of simulation

### B. Semi-Explicit DAE of Index 1

If at an equilibrium point, the system (1) is called semi-explicit [18], index-1 property requires that  $g(x_d, x_a)$  is solvable for  $x_a$  and  $\det(g_{x_a}(x_d, x_a)) \neq 0$  (to simplify  $x_d(t) = x_d, x_a(t) = x_a$ ):

$$\begin{cases} 0 = g_{x_d}(x_d, x_a)\dot{x}_d + g_{x_a}(x_d, x_a)\dot{x}_a \\ 0 = g_{x_d}(x_d, x_a)F_d(x_d, x_a, u) + g_{x_a}(x_d, x_a)\dot{x}_a \end{cases} \quad (5)$$

where  $g_{x_a}(x_d, x_a) = \frac{\partial g(x_d, x_a)}{\partial x_a}$  and  $g_{x_d}(x_d, x_a) = \frac{\partial g(x_d, x_a)}{\partial x_d}$

In other words, the differentiation index is 1, if, by differentiation of the algebraic equations with respect to time, an implicit ODE system results:

$$\begin{cases} \dot{x}_d = F_d(x_d, x_a, u) \\ \dot{x}_a = -g_{x_a}^{-1}(x_d, x_a)g_{x_d}(x_d, x_a)F_d(x_d, x_a, u) \end{cases} \quad (6)$$

where  $g_{x_a}^{-1}(x_d, x_a) \in \mathbb{R}^{n_a \times n_a}$  and  $g_{x_d}(x_d, x_a) \in \mathbb{R}^{n_a \times n_d}$ .

A study of nature and stability of DAE system is given by [19]. It should be noted that:

$$g_{x_a}(x_d, x_a) = \frac{\partial g(x_d, x_a)}{\partial x_a} = \begin{pmatrix} g_{x_a1} & g_{x_a2} \\ g_{x_a3} & g_{x_a4} \end{pmatrix} = [J] = \begin{pmatrix} j_1 & j_2 \\ j_3 & j_4 \end{pmatrix} \quad (7)$$

where :

- $[J]$  is the Jacobian matrix used in the Load Flow calculation excepted for generators terms, which allows us to verify that this  $\det(g(x_d, x_a)) \neq 0$  and  $g$  is solvable for any  $x_a$  (the elements of this matrix are the components of the diagonal Jacobian matrix used in load flow).
- $g_{x_a1} = \frac{\partial P}{\partial \theta} = P_\theta$ ,  $g_{x_a2} = \frac{\partial P}{\partial V} = P_V$ ,  $g_{x_a3} = \frac{\partial Q}{\partial \theta} = Q_\theta$ , and  $g_{x_a4} = \frac{\partial Q}{\partial V} = Q_V$ .

### C. Proposed Dynamic Power System Model

The basic idea is to extend the principle of decoupled algorithm used in Load Flow [3] and in SSE [2] to the dynamic model (and consequently to the DSE), but it apply only to the matrix  $g_{x_a}(x_d, x_a)$ . In the dynamic model (4), matrix  $g_{x_a}(x_d, x_a)$  is formed by the differentiation of the algebraic constraints to the algebraic states and formed by the same elements of Jacobean matrix which are used for load flow calculation. In an equilibrium point (or around), we assume that the variation of  $\dot{x}_a$  is very small and can be approximated, with the same methodology used in Newton's algorithm to load flow calculation (same principle), by  $x_a(n+1) = x_a(n) + \Delta x_a(n)$  where:

$$[\Delta x_a(n)] = \begin{bmatrix} \Delta \theta(n) \\ \Delta V(n) \end{bmatrix} = -g_{x_a}^{-1}(x_d, x_a)g_{x_d}(x_d, x_a) \begin{bmatrix} \Delta \delta \\ \Delta P(n) \end{bmatrix} \quad (8)$$

and  $\Delta P(n) \approx P_M(n) - P_G(n)$  and  $\Delta \delta = \omega - \omega_s$ . The solution  $x_a(t)$  should always verify that calculated by load flow (in permanent mode  $\dot{x}_a$  must be equal to 0 to verify the algebraic constraints). So we have the same formulation as that used for the load flow calculation and we can apply the principle of decoupled algorithms.

With the same reasoning, we applied a change only to the matrix  $g_{x_a}(x_d, x_a)$  in a similar way to that of the decoupled algorithm ( $g_{x_a}(x_d, x_a)|_{Dec}$ ):

$$\begin{aligned} \dot{x}_a &= -g_{x_a}^{-1}(x_d, x_a)g_{x_d}(x_d, x_a)F_d(x_d, x_a, u) \\ &= -g_{x_a}^{-1}(x_d, x_a)|_{Dec} g_{x_d}(x_d, x_a)F_d(x_d, x_a, u) \end{aligned} \quad (9)$$

We present in what follows the principle of decoupled algorithm used for load flow and SSE. Let us consider an electrical line model given at Fig. 3:

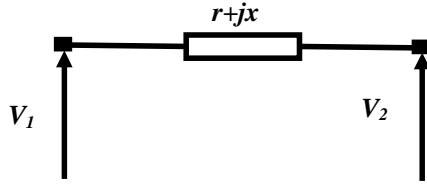


Fig. 3 Schema of electrical line

where the voltage  $V_1$  is supposed to be constant and the voltage  $V_2$  is taken as the origin of phase with  $r$  and  $x$  are respectively resistance and inductive reactance of line. We have:  $\Delta\theta = \frac{rQ_2 + xP_2}{V_2}$  and  $\Delta V = \frac{rP_2 + xQ_2}{V_2}$ . In a high voltage network, it is obvious that the phase ( $\theta$ ) depend primarily on the circulation of the active powers and that the modules of the nodal voltage ( $V$ ) are mainly dependent on the circulation of the reactive powers because  $r \ll x$ . In these conditions, we can approximate  $\Delta\theta$  and  $\Delta V$  by  $\frac{xP_2}{V_2}$  and  $\frac{xQ_2}{V_2}$  respectively.

These approximations allow us to cancel sub matrix  $[g_{x_2}]$  and  $[g_{x_3}]$ , therefore obtaining a reduced dimensions system [20]. We can thus write this matrix in the following simplified form:

$$g_{x_a}(x_d, x_a)|_{Dec} = \frac{\partial g(x_d, x_a)|_{Dec}}{\partial x_a} = \begin{pmatrix} g_{x_{a1}} & 0 \\ 0 & g_{x_{a4}} \end{pmatrix} \quad (10)$$

$$= [J]_{Dec} = \begin{pmatrix} j_1 & 0 \\ 0 & j_4 \end{pmatrix}$$

To validate the proposed dynamic decoupled model, we present the variation of the difference between the magnitude voltage  $V_2$  in load node 2 given respectively: by the diagram in Fig. 2, OM and DM for 3 buses test system:

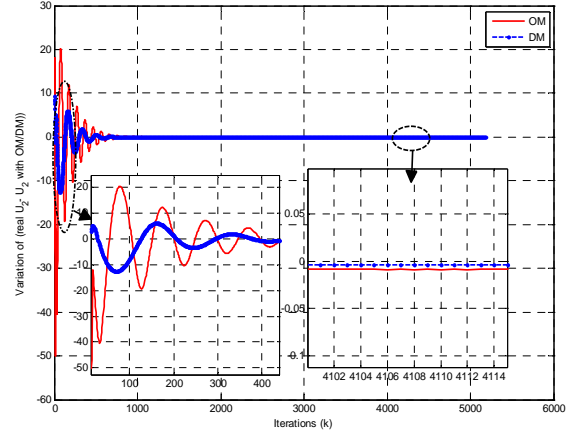


Fig. 4 Plots of  $V_2 - V_{2_{om}}$  and  $V_2 - V_{2_{dm}}$

Fig. 4 shows that the two models converge to the same value (found in load flow), but with DM it converges faster than the OM and there are no oscillations with important value during the first iterations with a very small error.

Now, we have tested the OM and proposed DM for 100 simulations while varying the initial values in a random way (variation of  $\pm 20\%$  with respect to the actual initial values). We put on Table I the relative error given by (11) where  $x_{real}$ ,  $x_{OM}$  and  $x_{DM}$  represent respectively the states generated by: diagram in Fig. 2, OM and the proposed DM.

$$\frac{\|x_{real} - x_{OM/DM}\|}{\|x_{real}\|} \quad (11)$$

TABLE I  
RELATIVE ERROR (%) AND COMPUTING TIME WITH RANDOM INITIAL VALUES

	OM	DM
Relative error	4.133 %	2.679%
Computing Time	1.72 s	1.24s

As we can see (line 2 of Table I), the proposed decoupled model (DM) converges with more accurate precision than with ordinary model (OM). Moreover, the results show that the computing time is better when using DM which permits to implement more effectively this model for real time application.

For the calculation of  $\dot{x}_a$ , the mathematical expressions are given in (12) for DM and in (13) for OM.

$$\dot{x}_a = \begin{bmatrix} \dot{\theta} \\ \dot{V} \end{bmatrix} = \begin{pmatrix} -P_{\theta_j}^{-1} P_{\delta_i} & 0 \\ -Q_{V_j}^{-1} Q_{\delta_i} & 0 \end{pmatrix} F_d(x_d, x_a, u) \quad (12)$$

where  $P_{\delta_i} = \frac{\partial P_j}{\partial \delta_i}$  and  $Q_{\delta_i} = \frac{\partial Q_j}{\partial \delta_i}$ .

$$\dot{x}_a = \begin{pmatrix} -P_{\theta_j}^{-1}P_{\delta_i} - T_1(P_{\delta_i} + Q_{\delta_i}) & 0 \\ -Q_{V_j}^{-1}Q_{\delta_i} + T_2 + T_3 & 0 \end{pmatrix} F_d(x_d, x_a, u) \quad (13)$$

where:

$$\begin{aligned} T_1 &= -P_{\theta_j}^{-1}P_{V_j}(Q_{V_j} - Q_{\theta_j}P_{\theta_j}^{-1}P_{V_j})^{-1} \\ T_2 &= Q_{V_j}^{-1}Q_{\theta_j}P_{\theta_j}^{-1}P_{\delta_i} \\ T_3 &= (I_{n_d/2} + Q_{V_j}^{-1}Q_{\theta_j}P_{\theta_j}^{-1}P_{V_j})^{-1}Q_{V_j}^{-1}Q_{\theta_j}P_{\theta_j}^{-1} \\ &\quad \cdot P_{V_j}Q_{V_j}^{-1}(Q_{\theta_j}P_{\theta_j}^{-1}P_{\delta_i} - Q_{\delta_i}) \end{aligned}$$

We note though, according to (12) and (13), that DM neglects some terms ( $T_1$ ,  $T_2$  and  $T_3$ ) used by OM (which reduces the computation time). These neglected terms can lead the system (during transient mode) to large values which decrease the response time (these terms can cause numerical instabilities which are shown by the difference of variation of the relative error in Table I).

Finally, the complete model in form ODE is according to:

$$\begin{aligned} \dot{x} &= \begin{pmatrix} \dot{x}_d \\ \dot{x}_a \end{pmatrix} = \bar{f}(x_d, x_a, u) \\ &= \begin{pmatrix} F_d(x_d, x_a, u) \\ -g_{x_a}^{-1}(x_d, x_a)g_{x_d}(x_d, x_a)F_d(x_d, x_a, u) \end{pmatrix} \\ \bar{y} &= \begin{pmatrix} 0 \\ y \end{pmatrix} = \bar{h}(x_d, x_a) = \begin{pmatrix} g(x_d, x_a) \\ h(x_d, x_a) \end{pmatrix} \end{aligned} \quad (14)$$

In the expression of  $\bar{h}(x_d, x_a)$ , the purpose of adding the algebraic constraint  $g(x_d, x_a)$  is to check it permanently (with OM:  $g_{x_a}$  and DM:  $g_{x_a}|_{Dec}$ ). It should be noted that the assumptions and the propositions given can be generalized for the other forms of dynamic power system models (models including a characteristic of the static/dynamic loads [21] and generators with exciter model [6]).

### III. DYNAMIC STATE ESTIMATION

The main problem in dynamic state estimation of power system is that few methods are applicable. Effectively, the numerous and strong nonlinearities in presence lead generally to the use of Extended Kalman Filter to resolve the state estimation problem. We propose here the Extended Kalman Estimator to increase the precision as well as the robustness of the estimation. A study of the convergence of EKF will be presented.

#### A. Extended Kalman Filter

The Kalman filter is a recursive estimator. It means that to consider the running state, only preceding state and current measurements are necessary. The history of the observations

and the estimates is; thus; not necessary. In the extended Kalman filter (EKF), the state transition and observation models need not be linear functions of the state but may instead be differentiable functions [22]. The considered nonlinear discrete system is given by (15):

$$\begin{cases} x_{k+1} = f(x_k, u_k) + v_k \\ y_k = h(x_k, u_k) + w_k \end{cases} \quad (15)$$

where  $v_k$  and  $w_k$  are the system and observation noises which are both assumed to be zero mean multivariate Gaussian noises with covariance  $Q_k$  and  $R_k$  respectively.

In this paper, we have used the classical form of EKF (we have used Euler discretization with a step size  $T_e$ ,  $x_{k+1} = x_k + T_e \bar{f}(x_k, u_k) = f(x_k, u_k)$  to discretize the continuous model (14)) given by:

$$\begin{aligned} \hat{x}_{k+1} &= f(\hat{x}_k, u_k) + K_k e_k \\ K_k &= F_k P_k H_k^T (H_k P_k H_k^T + R_k)^{-1} \\ P_{k+1} &= (F_k - K_k H_k) P_k F_k^T + Q_k \\ e_k &= y_k - h(\hat{x}_k, u_k) \end{aligned} \quad (16)$$

with:  $F_k = F(\hat{x}_k, u_k) = \frac{\partial(x_k + T_e \bar{f}(x_k, u_k))}{\partial x_k} \Big|_{x_k = \hat{x}_k}$  and

$$H_k = H(\hat{x}_k, u_k) = \frac{\partial \bar{h}(x_k, u_k)}{\partial x_k} = \begin{pmatrix} \frac{\partial g(x_k)}{\partial x_k} \\ \frac{\partial h(x_k)}{\partial x_k} \end{pmatrix} \Big|_{x_k = \hat{x}_k}$$

There are some attempts to apply Kalman Filter on linearized D.A.E system [23], but our proposition is to apply the E.K.E in the classic general form with some numerical approximations that we propose for the Jacobian calculation.

Initially, it should be noted that due to the difficulty of finding  $F_k$  (following the transformation of the algebraic variables in ODE model), we will make the following numerical approximation:

$$\begin{aligned} F_k &= F(\hat{x}_k, u_k) = \frac{\partial(x_k + T_e \bar{f}(x_k, u_k))}{\partial x_k} \Big|_{x_k = \hat{x}_k} \\ &= \left\{ \begin{array}{l} \frac{\partial(x_{d_k} + T_e F_d(x_{d_k}, x_{a_k}, u_k))}{\partial(x_{d_k}, x_{a_k})} \\ \frac{\partial(x_{a_k} + T_e (-g_{x_a}^{-1}(x_{d_k}, x_{a_k})g_{x_d}(x_{d_k}, x_{a_k})F_d(x_{d_k}, x_{a_k}, u_k)))}{\partial(x_{d_k}, x_{a_k})} \end{array} \right\} \quad (17) \end{aligned}$$

The numerical approximation is used on the second term of  $F_k$  (since it is very difficult to determine) as follows:

$$\frac{\partial(x_{d_k} + T_e(-g_{x_a}^{-1}(x_{d_k}, x_{a_k})g_{x_d}(x_{d_k}, x_{a_k})F_d(x_{d_k}, x_{a_k}, u_k)))}{\partial(x_{d_k}, x_{a_k})} \quad (18)$$

$$\approx (I_{n_a} + T_e(-g_{x_a}^{-1}(x_{d_k}, x_{a_k})g_{x_d}(x_{d_k}, x_{a_k})\frac{\partial F_d(x_{d_k}, x_{a_k}, u_k)}{\partial(x_{d_k}, x_{a_k})}))$$

For  $x_{d_k} = \hat{x}_{d_k}$ ,  $x_{a_k} = \hat{x}_{a_k}$ . The terms  $g_{x_a}^{-1}$  and  $g_{x_d}$  are calculated numerically.

### B. Convergence Analysis

In this section, we present a convergence analysis of EKF (16) based on the method of [24], [25] and [26] by including an unknown diagonal matrix to model linearization errors and a Lyapunov function. This leads to the resolution of a LMI which depends on the choice of  $R_k$  and  $Q_k$ . Initially, the error vector is defined:  $\tilde{x}_k = x_k - \hat{x}_k$  and the candidate Lyapunov function is:  $V_{k+1} = \tilde{x}_{k+1}^T P_{k+1}^{-1} \tilde{x}_{k+1}$ , where:

$$\begin{cases} \tilde{x}_{k+1} = \alpha_k (F_k - K_k H_k) \tilde{x}_k = \alpha_k \tilde{F}_k \tilde{x}_k \\ P_{k+1}^{-1} = (\tilde{F}_k P_k F_k^T + Q_k^c)^{-1} \\ \alpha_{jk} = \text{diag}(\alpha_{1k}, \dots, \alpha_{(n_d+n_a)k}) \end{cases}$$

We have then:

$$V_{k+1} = (\alpha_k \tilde{F}_k \tilde{x}_k)^T P_{k+1}^{-1} (\alpha_k \tilde{F}_k \tilde{x}_k) \quad (19)$$

$$= \tilde{x}_k^T \tilde{F}_k^T \alpha_k (\tilde{F}_k P_k F_k^T + Q_k^c)^{-1} \alpha_k \tilde{F}_k \tilde{x}_k$$

A decreasing sequence  $\{V_k\}_{k=1, \dots}$  means that there exists a positive scalar  $0 < \xi < 1$  so that:  $V_{k+1} - (1 - \xi)V_k \leq 0$ . This gives us this LMI:

$$\tilde{F}_k^T \alpha_k (\tilde{F}_k P_k F_k^T + Q_k^c)^{-1} \alpha_k \tilde{F}_k - (1 - \xi)P_k^{-1} \leq 0 \quad (20)$$

With the same reasoning used in [24], we determine domains in which (20) is satisfactory. Under the following assumption:

$$|\alpha_{jk}| \leq \bar{\alpha}_k = \sup_j |\alpha_{jk}| \leq \left( \frac{(1 - \xi)\underline{\sigma}(\tilde{F}_k P_k F_k^T + Q_k^c)}{\bar{\sigma}(F_k^T)\bar{\sigma}(P_k)\bar{\sigma}(\tilde{F}_k)} \right)^{\frac{1}{2}} \quad (21)$$

$\{V_k\}_{k=1, \dots}$  is a decreasing sequence. With  $\underline{\sigma}$  and  $\bar{\sigma}$  denoting the maximum and minimum singular values respectively, and as  $\alpha_k$  is a diagonal matrix then:

$$[\bar{\sigma}(\alpha_k)]^2 \leq \frac{(1 - \xi)\underline{\sigma}(\tilde{F}_k P_k F_k^T + Q_k^c)}{\bar{\sigma}(F_k^T)\bar{\sigma}(P_k)\bar{\sigma}(\tilde{F}_k)} \quad (22)$$

$$\leq \frac{(1 - \xi)\underline{\sigma}(P_k^{-1})}{\bar{\sigma}(\tilde{F}_k^T)\bar{\sigma}((\tilde{F}_k P_k F_k^T + Q_k^c)^{-1})\bar{\sigma}(\tilde{F}_k)}$$

We have then:

$$\bar{\sigma}(\tilde{F}_k^T \alpha_k (\tilde{F}_k P_k F_k^T + Q_k^c)^{-1} \alpha_k \tilde{F}_k) \leq [\bar{\sigma}(\alpha_k)]^2 \bar{\sigma}(\tilde{F}_k^T)\bar{\sigma}((\tilde{F}_k P_k F_k^T + Q_k^c)^{-1})\bar{\sigma}(\tilde{F}_k) \leq (1 - \xi)\underline{\sigma}(P_k^{-1}) \quad (23)$$

When (23) is satisfied,  $V_k$  is a strictly decreasing sequence. This last equation gives us an idea on the choice of  $Q_k^c$  and for  $R_k^c$ , we proceed as follows:

$$\bar{\sigma}(\tilde{F}_k) = \bar{\sigma}(F_k - K_k H_k) = \bar{\sigma}(F_k - F_k P_k H_k^T (H_k P_k H_k^T + R_k^c)^{-1} H_k) \quad (24)$$

$$= \bar{\sigma}[F_k (I_{n_a+n_d} - P_k H_k^T (H_k P_k H_k^T + R_k^c)^{-1} H_k)]$$

by replacing  $P_k H_k^T (H_k P_k H_k^T + R_k^c)^{-1} H_k$  by  $A_k$ , we obtain:

$$\bar{\sigma}(\tilde{F}_k) \leq \bar{\sigma}(F_k) \bar{\sigma}[A_k (A_k^{-1} + I_{n_a+n_d})] \leq \bar{\sigma}(F_k) \bar{\sigma}(A_k) \bar{\sigma}(A_k^{-1} + I_{n_a+n_d}) \quad (25)$$

with

$$\bar{\sigma}(A_k) \leq \bar{\sigma}(P_k H_k^T) \bar{\sigma}((H_k P_k H_k^T + R_k^c)^{-1} H_k) \leq \bar{\sigma}(P_k H_k^T) \bar{\sigma}((H_k P_k H_k^T + R_k^c)^{-1}) \bar{\sigma}(H_k) \leq \frac{\bar{\sigma}(P_k H_k^T) \bar{\sigma}(H_k)}{\underline{\sigma}(H_k P_k H_k^T + R_k^c)} \quad (26)$$

We obtain finally:

$$\bar{\sigma}(\tilde{F}_k) \leq \frac{\bar{\sigma}(F_k) \bar{\sigma}(P_k H_k^T) \bar{\sigma}(H_k) \bar{\sigma}(A_k^{-1} + I_{n_a+n_d})}{\underline{\sigma}(H_k P_k H_k^T + R_k^c)} \quad (27)$$

For example, we can choose  $Q_k^c$  sufficiently large and  $R_k^c$  so that (27) is satisfied, thus  $\alpha_k$  may be large and not necessarily very close to identity matrix. However, in order to ensure  $\lim_{k \rightarrow \infty} (x_k - \hat{x}_k) = 0$  and since  $V_k$  is a strictly decreasing sequence and  $P_k$  is a bounded matrix, it follows that:

$$0 \leq \mu \tilde{x}_k^T \tilde{x}_k \leq V_k \leq (1 - \xi)^k V_0 \Rightarrow 0 \leq \mu \lim_{k \rightarrow \infty} (\tilde{x}_k^T \tilde{x}_k) \leq \lim_{k \rightarrow \infty} (V_k) \leq V_0 \lim_{k \rightarrow \infty} ((1 - \xi)^k) = 0$$

with  $0 \leq \mu I_{n_d+n_a} \leq P_k^{-1}$ .

Consequently, in the same reasoning of [24] and [26], and so that the EKF ensures local asymptotic convergence, we must verify the following conditions:

1. System (15) is  $M$ -locally uniformly rank observable, there exists  $k \geq M - 1$  where the observability matrix:

$$\text{rank}(O(k-M+1, k)) = (n_d + n_a) \quad (28)$$

where

$$O(k-M+1, k) = \begin{bmatrix} H_{k-M+1} \\ H_{k-M+2}F_{k-M+1} \\ \dots \\ H_k F_{k-1} \dots F_{k-M+1} \end{bmatrix}$$

In practice, we use a numerical rank test on  $O(k-M+1, k)$ .

2.  $F_k$ ,  $H_k$  are uniformly bounded matrices and  $F_k^{-1}$  exist.
3. The matrices  $Q_k^c$  and  $R_k^c$  are chosen so that the bounds (22) and (27) are satisfied:

$$\begin{aligned} Q_k^c &= \eta e_k^T e_k I_{n_d+n_a} + \nu I_{n_d+n_a} \\ R_k^c &= \epsilon H_k P_k H_k^T + \mu I_m \end{aligned} \quad (29)$$

where  $\eta$  and  $\nu$  are to be chosen large and positive and  $\epsilon$  and  $\mu$  a positive scalar fixed by the user. Indeed, once the convergence is reached (using the output error vector as a criterion) we switch to the actual covariance matrices i.e.  $Q_k^c = Q_k$ ,  $R_k^c = R_k$ .

#### IV. SIMULATION RESULTS

Studies are carried out on the IEEE 13 buses test system to evaluate the performance of the dynamic state estimation of the proposed model on a Pentium Dual-Core, 1.60 GHz Personal Computer. The transit power is considered as measurements which are generated by the diagram of simulation given in Fig. 2. For the discretization of the model (14), we used Euler discretization with a step size  $T_e = 10^{-4}$  s.

The network includes:

- 5 generator buses: 2, 5, 7, 11 and 12 (with node 12 taken as the reference bus) and 8 static load nodes: 1, 3, 4, 6, 8, 9, 10 and 13.
- The outputs are the transit powers between nodes 7 and 6 ( $P_{7,6}$ ) and nodes 12 and 1 ( $P_{12,1}$ ) with a state vector composed by 24 variables ( $[x] = [\delta_i \omega_i \theta_j V_j]^T$  with  $i=2, 5, 7, 11$  and  $j=1, 3, 4, 6, 8, 9, 10, 13$ ).

Firstly, we present the evolution of the reciprocal condition estimator  $rcond(O_{13buses}^{(k-13,k)})$  in Fig. 5 to verify the observability.

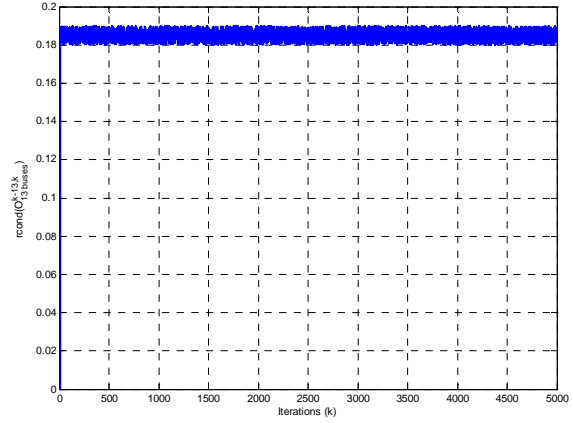


Fig. 5 Evolution of  $rcond(O_{13buses}^{(k-13,k)})$

After the verification of the observability,  $O_{13buses}^{(k-13,k)}$  is well conditioned ( $rcond(O_{13buses}^{(k-13,k)}) > 0$ ), the measurements are the results of the diagram of simulation (Fig. 2) and by applying low variance noise to the measurements ( $w_k = \pm 5\%$  of real value) with:

$$\begin{aligned} Q_k^{EKF} &= 2.753 * 10^{-5} I_{24} \\ R_k^{EKF} &= \begin{pmatrix} 0.015664 & 0 \\ 0 & 0.014307 \end{pmatrix} \end{aligned}$$

We show in Fig. 6 the variation of the estimated bus voltage in node 1 ( $\hat{x}_{17}$ ) with OM and DM (we used the final value (constant final value = 201.45 kV) to show the variation in the transient mode):

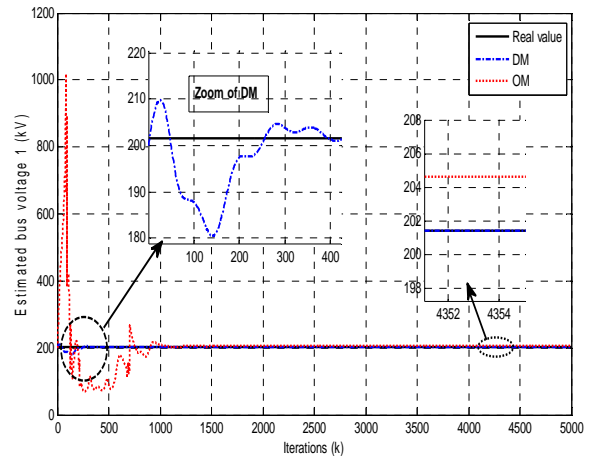


Fig. 6 Evolution of the estimated bus voltage:  $\hat{V}_1(k)$  with OM and DM

It is clear, according to Fig. 6, that the estimated bus voltage ( $\hat{V}_1(k)$ ) converges to the real value with a small error

(which is due to the addition of disturbance on measures) with DM, error equal to 0.02. However with OM it's equal to 0.18. The reason why non-zero error is obtained after the estimation process comes from the fact that the measurements are corrupted by a disturbance ( $\pm 5\%$  of real value).

While noting that with the DM, the variation is more stable in transient mode because the elimination of the added elements  $P_V$  and  $Q_\theta$  with OM. This is verified by:

First, the variation of Condition number of additive terms  $T_1$  and  $T_2+T_3$  in OM (neglected with the DM), where a disturbance is injected between iterations 2500 and 2510 (we reset the phases  $\theta_j$ ).

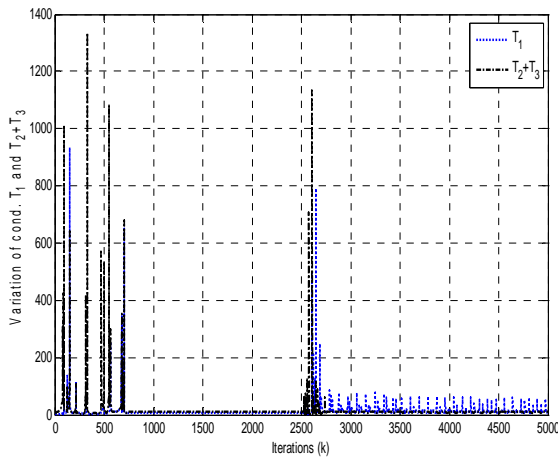


Fig. 7 Evolution of  $T_1$  and  $T_2+T_3$  in OM

The results obtained in Fig. 7 shows that, in the first iterations (transient mode), a large condition numbers of these terms indicates a nearly singular matrix, especially when a disturbance is injected. The existence of a singular matrix during the first iterations causes a peak value (which reduces the response time) and might lead the system to diverge.

Second, by:

- The variation of  $\hat{V}_1(k)$  with OM (variation of 395% of finale value) and DM (just a small variation of 7.42%).
- The number of iterations until convergence: with OM after 1000 iterations and only 400 iterations with DM.

Concerning the last point, it is due to the fact that with DM, we have to invert only two matrices of a dimension of  $8 \times 8$  (each matrix is formed by 12 elements). However with OM a matrix of  $16 \times 16$  (matrix formed by 48 elements) to calculate only  $g_{x_d}(x_d, x_a)^{-1}$ .

Third, by the evolution of the relative error given by (11) (using the same conditions as Table I) with OM and DM.

TABLE II  
RELATIVE ERROR (%) AND COMPUTING TIME WITH RANDOM INITIAL VALUES

	OM	DM
Relative error	6.857%	3.819%
Computing Time	121.2s	98.016s

Table II shows that the proposed decoupled model converges with more accurate precision than ordinary model (with DM 3.819%, however with OM 6.857%). We notice, also, that the computing time with DM (98.016s) gives an indication on the feasibility and the possibility of practical implementation.

Now, the measurement values are generated by adding high variance noise to the measurements ( $w_k = \pm 15\%$  of real value). We present the evolution of the norm of error estimation by OM and DM:  $\|x^{real} - \hat{x}\|$  (respectively Figs. 8 and 9) with the previous values of  $Q_k^c$  and  $R_k^c$  (Standard EKF) and these new values (Modified EKF: proposed choice given in III-B by (29)):

$$Q_k^{EKF} = 10^{10} e_k^T e_k I_{24} + 10^{-3} I_{24}$$

$$R_k^{EKF} = 10 H_k P_k H_k^T + 10^{-3} I_2$$

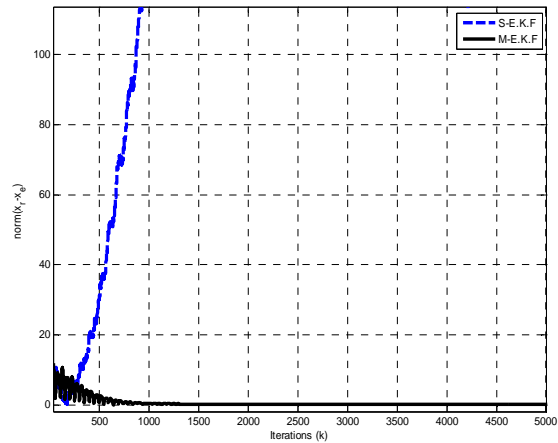


Fig. 8 Evolution of  $\|x^{real} - \hat{x}\|$  with OM

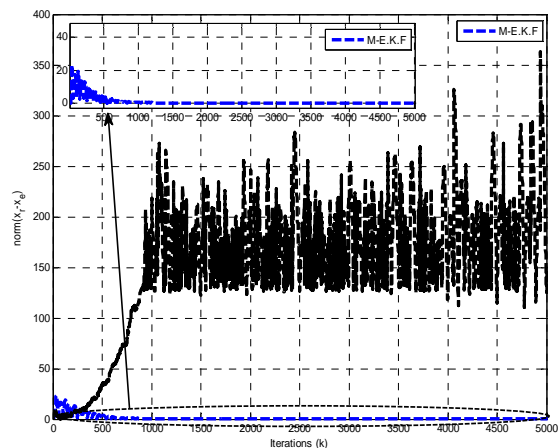


Fig. 9 Evolution of  $\|x^{real} - \hat{x}\|$  with DM

Concerning the evolution of error estimation, the results show that the appropriate choice of matrices  $Q_k^c$  and  $R_k^c$  given by (29) insures the convergence of the estimated states



to the real value with OM (in Fig 8, we used a zoom to show the evolution of the estimation error since the error with the S-EKF completely diverges) and DM. Another problem connected to the stability of DSE methods is the choice of initial values for various states. We tested the Standard and Modified EKF (respectively S-EKF and M-EKF) for 100 simulations while varying the initial values in a random way (variation of  $\pm 20\%$  with respect to the actual initial values) with OM and DM. The following Table III shows the % of convergence by applying a disturbance to the system parameters:

- Case 1: Adding a low variance noise to the system (variation of  $v_k = \pm 5\%$  applied on  $G_{ij}$  and  $B_{ij}$ ).
- Case 2: Adding a high variance noise to the system (variation of  $v_k = \pm 15\%$  applied on  $G_{ij}$  and  $B_{ij}$ ).

TABLE III  
CONVERGENCE (%) WITH RANDOM INITIAL VALUES

Estimator	OM (Case 1)	DM (Case 1)	OM (Case 2)	DM (Case 2)
S-EKF	47%	52%	45%	48%
M-EKF	90%	94%	88%	91%

In the general case, the studied algorithms converge to the good values only when they are initialized  $\pm$  near their actual values (the voltages are selected close to the values of the generator voltages and the phases equal to 0). Table III shows clearly that the Modified EKF converges in the majority of the cases compared with the Standard version and especially with the proposed DM.

We present now in Table IV the relative error given by (30) when we add high variance noise to the measurements ( $\pm 15\%$  of real value) with the same previous conditions on initial values.

$$\frac{\|x_{real} - \hat{x}_{OM/DM}\|}{\|x_{real}\|} \quad (30)$$

TABLE IV  
RELATIVE ERROR (%) WITH RANDOM INITIAL VALUES

Relative error	OM	DM
S-EKF	43.43%	28.73%
M-EKF	8.89%	4.86%

The values obtained in Table IV confirm that the M-EKF increases the estimation quality. In fact, with the use of M-EKF with the proposed DM, the relative error is reduced by 5.91 times in comparison with S-EKF.

It should be noted that the results of simulation of dynamic model given by the diagram (Fig. 2) are validated and compared with those generated by the Toolbox *SimPowerSystems* of *MATLAB*® (we obtained the same results). In addition, the use of this Toolbox facilitates the real time implementation in DSP device.

## V. CONCLUSION

An efficient decoupled dynamic power system model has been described and investigated based on introducing a transformation of ordinary DAE model using decoupled algorithm. We also used the classical method of EKF to dynamic state estimation of power systems including some numerical approximation for the calculation of the Jacobian matrix and which was preceded by a convergence analysis. The results show well the appropriate choice of the dynamic DM in terms of robustness, speed and computing time and, in a very clear way, the high quality of estimation offered by the Modified EKF. The remaining open questions are the experimental test of the proposed method and its application to large scale power test systems using the decentralized state estimation approaches for each zone (for each zone we apply the EKF with the DM) with coordination techniques to reduce the computational requirements. These two issues will be investigated in the near future.

## REFERENCES

- [1] N.R. Shivakumar and A. Jain, "A review of power system dynamic state estimation techniques," in *Power Syst. Technology and IEEE Power India Conf.*, New Delhi, India, 2008, pp.1-6.
- [2] R. Neela and P. Aravindhababu, "A new decoupling strategy for power system state estimation," *Int. J. of Energy Convers. and Management*, vol.50, pp.2047-2051, 2009.
- [3] A. Thabet, S. Chniba, D. Gaetan, M. Boutayeb and M.N. Abdelkrim, "Power systems load flow and state estimation: Modified methods and evaluation of stability and speeds computing." *Int. Rev. of Electr. Eng.*, vol.5, pp.1110-1118, 2010.
- [4] E. Scholtz, "Observer based monitors and distributed wave controllers for electromechanical disturbances in power systems," Ph.D. dissertation, Massachusetts Institute Technology, USA, 2004.
- [5] M.A. Pai, P.W. Sauer, B.C. Lesieutre and R. Adapa, "Structural stability in power systems-effect of load models," *IEEE Trans. on Power Syst.*, vol.10, pp.609-615, 1995.
- [6] C.J. Dafis, "An observability formulation for nonlinear power systems modeled as differential algebraic systems," Ph.D. dissertation, Drexel university, PA, USA, 2005.
- [7] A.S. Debes and R.E. Larson, "A dynamic estimator for tracking the state of a power system." *IEEE Trans. on Power App. And Syst.*, vol.89, pp.1670-1678, 1970.
- [8] J. Aslund and E. Frisk, "An observer for nonlinear differential-algebraic systems," *Automatica*, vol.42, pp.959-965, 2006.
- [9] T. Wichmann, "Simplification of nonlinear DAE systems with index tacking," in *European Conf. on Circuit Theory and Design*, Espoo, Finland, 2001, pp.173-176.
- [10] R. Nikoukhah, A. Willsky and B. Levy, "Kalman filtering and riccati equations for descriptor systems," *IEEE Trans. on Autom. Control*, vol.37, pp.1325-1342, 1992.
- [11] M.F. Isabel and F.P. Barbosa, "Square root filter algorithm for dynamic state estimation of electric power systems," in *Electrotechnical Conference, 7th Mediterranean*, Antalya, Turkey, 1994, pp.877-880.
- [12] K. Shih and S. Huang, "Application of a robust algorithm for dynamic state estimation of a power system." *IEEE Trans. on Power Syst.*, vol.17, pp.141-147, 2002.
- [13] K.Yu, N. Watson and J. Arrillaga, "An adaptive Kalman filter for dynamic harmonic state estimation and harmonic injection tracking," *IEEE Trans. on Power Delivery*, vol.20, pp.1577-1584, 2005.
- [14] H. Ma and A. Grigis, "Identification and tracking of harmonic sources in a power system using Kalman filter," *IEEE Trans. on Power Delivery*, vol.11, pp.1659-1665, 1996.
- [15] H. Beids and G. Heydt, "Dynamic state estimation of power system harmonics using kalman filter methodology," *IEEE Trans. on Power Delivery*, vol.6, pp.1663-1670, 1991.

- [16] F. Chowdhury, J. Christensen and J. Aravena, "Power system fault detection and state estimation using Kalman filter with hypothesis testing," *IEEE Trans. on Power Delivery*, vol.6, pp.1025–1030, 1991.
- [17] Roytelman and S. Shahidehpour, "State estimation for electric power distribution systems in quasi real-time conditions," *IEEE Trans. on Power Delivery*, vol.8, pp.2009–2015, 1993.
- [18] B.W. Gordon, "Dynamic sliding manifolds for realization of high index differential-algebraic systems," *Asian J. of Control*, vol.5, pp.454–466, 2003.
- [19] D.C. Tarraf and H.H. Asada, "On the nature and stability of differential-algebraic systems," in *Proc. American Control Conf.*, Anchorage, USA, 2002, pp.3546–3551.
- [20] M. Eremia, J. Trecat and A. Germond, "*Réseaux électriques: Aspects Actuels*, 2<sup>nd</sup> ed. Bucuresti, Editura Tehnica, 2000.
- [21] D. Karlsson and D.J. Hill, "Modelling and identification of nonlinear dynamic loads in power systems," *IEEE Trans. on Power Syst.*, vol.9, pp.157–166, 1994.
- [22] K. Judd, "Nonlinear state estimation in distinguishable states and the extended Kalman filter," *Physica D: Nonlinear Phenomena*, vol.183, pp.273–281, 2003.
- [23] V.M. Becerra, P.D. Roberts and G.W. Griffiths, "Applying the extended Kalman filter to systems described by nonlinear differential-algebraic equations," *Control Eng. Practice*, vol.9, pp.267–281, 2001.
- [24] M. Boutayeb and C. Aubry, "A strong tracking extended Kalman observer for nonlinear discrete-time systems," *IEEE Trans. on Autom. Control*, vol.44, pp.1550–1556, 1999.
- [25] M. Boutayeb, "Identification of nonlinear systems in the presence of unknown but bounded disturbances," *IEEE Trans. on Autom. Control*, vol.45, pp.1503–1507, 2000.
- [26] Y. Song and J. Grizzle, "The extended kalman filter as a local asymptotic observer for non linear discrete-time systems," *J. of Math. Syst. Estimation and Control*, vol.5, pp. 59–78, 1995.